ORIGINAL RESEARCH

Irradiation-Induced Activated Microglia Affect Brain Metastatic Colonization of NSCLC Cells via miR-9/*CDH1* Axis

Yu Jin[1]
Yalin Kang[1]
Xiaohong Peng[1]
Li Yang[2]
Qianxia Li[1]
Qi Mei[1]
Xinyi Chen[1]
Guangyuan Hu[1]
Yang Tang[1]
Xianglin Yuan[1]

[1]Department of Oncology, Tongji Hospital, Tongji Medical College, Huazhong University of Science and Technology, Wuhan, Hubei Province, People's Republic of China; [2]Department of Hematology, Tongji Hospital, Tongji Medical College, Huazhong University of Science and Technology, Wuhan, Hubei Province, People's Republic of China

Background and Purpose: Brain metastasis is among the leading causes of death in patients with non-small-cell lung cancer (NSCLC). Through yet unknown mechanisms, prophylactic cranial irradiation (PCI) can significantly decrease the incidence of brain metastases. Given that PCI probably exerts indirect anti-tumoral effects by turning cerebral "soil" unfavorable for the colonization of metastatic tumor "seeds". This study aims to reveal how PCI regulates the brain microenvironment conducing to a reduction in brain metastases.

Materials and Methods: Key markers of M1/M2 microglia types and mesenchymal-to-epithelial transition (MET) were analyzed by qRT-PCR and Western Blot in vitro. The target miR-9 was obtained by miRNA array analysis and confirmed by qRT-PCR in microglia. We used miRTarBase and TargetScan to analyze the target genes of miR-9 and confirmed by luciferase activity assay. Anti-metastatic effects of irradiation on the brain were evaluated by intravital imaging using a brain metastatic A549-F3 cell line in a nude mouse model.

Results: Irradiation induced M1 microglia activation, which inhibited the MET process of A549 cell lines. Furthermore, levels of miR-9 secreted by irradiated M1 microglia significantly increased and played a vital role in the inhibition of the A549 MET process by directly targeting *CDH1*, concurrently decreasing cell capacity for localization in the brain, thus reducing brain metastases.

Conclusion: We demonstrated that miR-9 secreted by irradiated M1-type microglia played an important role in modulating A549 cell lines into mesenchymal phenotype and further decreased their localization capabilities in the brain. Our findings signify the modulating effect of irradiation on metastatic soil and the cross-talk between tumour cells and the metastatic microenvironment; importantly, they provide new opportunities for effective anti-metastasis therapies, especially for brain metastasis patients.

Keywords: non-small-cell lung cancer, brain metastasis, cranial irradiation, microglia, miR-9

Introduction

Lung cancer is among the leading causes of premature mortality worldwide, accounting for over 142,670 cancer-related deaths in the United States in 2019.[1,2] Metastasis is the main cause of death in lung cancer patients; while brain metastasis (BM) being common among both small-cell lung cancer (SCLC) and non-small cell lung cancer (NSCLC) patients.[3] It is estimated that 20%–56% of patients with advanced lung cancer would experience brain metastases, accounting for 40%–50% of all brain metastases.[4,5] Despite recent progress in diagnosis and treatment of BM, the associated overall median survival remains less than 6 months.[6] Prophylactic

Correspondence: Yang Tang;
Xianglin Yuan
Department of Oncology, Tongji Hospital, Tongji Medical College, Huazhong University of Science and Technology, 1095 Jiefang Avenue, Wuhan, Hubei Province, China
Tel +86-27-83663342
Email tangyangtjmu@126.com;
yuanxianglin@hust.edu.cn

cranial irradiation (PCI) was introduced in 1980 as a method to prevent brain metastasis.[7] Randomized clinical trials and a meta-analysis have shown that PCI was concerned with improved survival in patients with SCLC.[8,9] As for NSCLC patients, the RTOG 0214 trial demonstrated that the incidence of BM was lower in the PCI (7.7%) than in the non-PCI group (18%) but there is no overall survival benefit.[10] However, the fundamental molecular mechanism of PCI in reducing brain metastasis remains to be fully elucidated.

Furthermore, the irradiation dosage used in PCI (usually <25 Gy in total) is insufficient to have tumoricidal effects. Therefore, accounting for the persistent protective effect months after PCI treatment remains challenging. Recent findings suggested that irradiation has a modulating effect on the brain local immune system.[11,12] In fact, studies have demonstrated that immune microenvironmental change in a distant organ can influence the rate of colonization of metastatic tumor cells.[13,14] Based on these results, our group proposed that PCI might alter the brain microenvironment ("soil") protecting it against the colonization of tumor ("seed"). Microglia, a resident macrophage, is a major constituent of the brain immune system, playing a vital role in the cerebral microenvironment.[15] Presence of different microglia phenotypes, including M1 and M2, has been previously proposed.[16,17] Moreover, it has been shown that under LPS stimulation, microglia turn into M1 type and exhibit a pro-inflammatory phenotype, which leads to tumor growth inhibition.[18,19] While microglia produce an M2-phenotype under activation of IL4 and IL10 to exert immune response-suppressive effect and create a microenvironment favorable to tumor proliferation.[20]

Studies on metastases have demonstrated that lung cancer cells affect several vital pathways, including those associated with evading immune system surveillance and developing chemotherapy resistance, both of which can facilitate metastatic behavior and disease progression.[21,22] Notably, during the metastatic process, tumor cells undergo a morphological change that involves in regulating multiple adhesion and cellular matrix molecules to acquire a mesenchymal phenotype. This phenomenon, called epithelial-to-mesenchymal transition (EMT), dramatically increases the rates of extravasation, blood/lymphatic vessel invasion, and distant organ reach of tumor cells.[23–25] When metastatic tumor cells travel to a distant organ, the reverse process occurs, mesenchymal-to-epithelial transition (MET), enabling these cells to up-regulate the expression of various adhesion molecules, localizing then in proximity and forming metastatic loci.[26] Meanwhile, studies indicate that microRNA plays an important role in the regulation of the EMT/MET process.[27] To explore the detailed MET inhibitory mechanism of irradiated M1 microglia on A549 cells, we performed a meta-study on microRNA expression by profiling a murine microglia cell model.

Therefore, we hypothesized that irradiated microglia might alter the phenotypical transition process and distant organ localization of tumor cells, which in turn lower the chances of brain metastasis. Here, we aimed to discover the polarization effect of irradiation on microglia, and to further explore the underlying mechanism of the inhibitory effects of microglia on tumor cell MET transition after ionized irradiation treatment.

Materials and Methods
Cell Lines and Irradiation Treatment

Human microglia cell lines CHME-5 and HMO6, human renal epithelial 293T cells, two human lung cancer cell lines A549 used in our study were purchased from Cell Bank, Chinese Academy of Sciences, China. The brain metastatic A549-F3 cells were derived from parental A549 cells, and the human glioma cell line U87 (authenticated STR profile shown in Supplementary Figure 1) was obtained from the oncology laboratory of Tongji Hospital, Wuhan, China. All the use of the cell lines was approved by ethics committee of Tongji Medical Collage, Huazhong University of Science and Technology (Wuhan, China). Cells were separately cultured in DMEM and RPMI 1640 medium (HyClone, Logan, UT), supplemented with 10% FBS (Gibco, Grand Island, NY), and maintained in a humidified incubator with 5% CO_2 at 37 °C. The mesenchymal phenotype of A549 cells was induced with recombinant human TGF-β1 (PeproTech; 100–21C). Cells were irradiated using an RS2000 X-ray Biological Research Irradiator (25 mA, 160 kV; Rad Source Technologies Inc., Suwanee, GA).

Western Blot Analysis

Cells were lysed using radioimmunoprecipitation assay (RIPA; Beyotime, Shanghai, China) buffer supplemented with protease inhibitor cocktail (MedChemExpress Thermo Scientific, USA) and phosphatase inhibitor (the Promoter Biotechnology, Wuhan, China) (100:1:1). The total protein concentration measured by BCA Protein Assay Kit

(AR0197; Boster, Wuhan, China). All protein samples were mixed in a 4:1 ratio (v/v) with 5* SDS loading buffer and heated at 100 °C for 5 min. Total equal protein (50 μg) were separated by SDS-PAGE gels and transferred to 0.45-μm (polyvinylidene fluoride membranes) PVDF membranes (Millipore, Billerica, USA). The membranes were subsequently incubated with 5% non-fat milk in TBST (TRIS-buffered saline and 2.5% Tween-20) for 1 hour at room temperature. Then, each membrane was incubated with specific primary antibodies overnight at 4 °C. These primary Abs included iNOS (1:1000, ab32101; Abcam), Arg1 (1:1000; Cell Signaling Technology, #93668), E-Cadherin (1:100; Abcam; ab1416), vimentin (1:1000; Abcam; ab8978), GAPDH (1:8000; Boster, BM1985), and α-tubulin Ab (1:2000, 11224-1-AP; Proteintech). The membranes were tested with an ECL detection system (Thermo Fisher Scientific, Waltham, MA).

Immunofluorescence

Briefly, CHME5 cells were seeded on glass slides and fixed with 4% paraformaldehyde. After cell attachment, slides were incubated with a primary antibody specific to iNOS (1:50, 18985-1-AP; Proteintech) overnight at 4 °C, followed by Cy3-conjugated secondary antibody for 1 hour. Later, cell nuclei were stained with DAPI for 5 minutes (Promoter, Wuhan, China). Immunofluorescence was captured under a fluorescence microscope (DMI3000B; Leica Microsystems, Shanghai, China) and qualitatively analyzed by ImageJ software.

Quantitative Real-Time PCR

Quantitative RT-PCR was conducted as described previously.[28] The primers used for GAPDH, Arg1 (The result of agarose gel electrophoresis for ARG1 was shown in Supplementary Figure 1), iNOS and IL1B are listed in Supplementary Table 1. To analyze miRNA expression, we used miDETECT A Track miRNA qRT-PCR Kit and a Bulge-Loop miRNA qRT-PCR Kit (RiboBio, Guangzhou, China) for reverse-transcribed, according to the manufacturer's introduction. Expression levels of miRNA were normalized to those of U6-snRNA expression while mRNA of IL-10, IL1B and iNOS were normalized to GAPDH expression. All experiments were performed in triplicate.

MicroRNA Array Analysis

Microarray data were retrieved from Freilich[18] and Gene Expression Omnibus (GEO, http://www.ncbi.nlm.nih.gov/geo, accession number GSE49330). Analytical pipeline was established according to the description by Yang et al.[29] Raw gene-chip data (gene chip type Mouse GeneChip miRNA 2.0 Array) were downloaded and analyzed with J-Express software package (Version 2012, Department of Informatics, University of Bergen, Norway). Chip data were calculated with the robust multichip analysis (RMA) to form datasets of log2-transformed probe set values. Genes significantly different in expression level were identified by the SAM method (FDR <1%), and data with group fold change >4 or ≤4 were extracted and analyzed with unsupervised hierarchical clustering (Pearson correlation).

Plasmid Transduction

We purchased negative control oligonucleotides plasmid (GV250), mimics of miR-9 plasmid (GMUE86649) and miR-9 inhibitor plasmid (GMDE86674) from GeneChem (Shanghai, China). A549 cells and A549-F3 cells were transfected with oligonucleotides using Lipofectamine 2000 reagent (11668–019, Invitrogen), according to the manufacturer's instructions. After 48h transfection, the efficiency was determined by fluorescence photography and quantitative RT-PCR.

Luciferase Activity Assay

We found cadherin 1 (also known as *CDH1*) was a potential target of miR-9 using TargetScan and miRTarBase software. Luciferase reporter assays were performed as described in the manufacturer's protocol. In short, the pMIR-REPORT-*CDH1*-3′UTR(WT) or pMIR-REPORT-*CDH1*-3′UTR(MUT) and miR-9-5p or scramble miRNA mimic were transfected into 293T cells. After co-transfection for 48h, luciferase activities were measured by Dual-Luciferase Reporter Assay System (E1910, Promega), using a fluorescence microscope (MHG-100B, MOTIC).

Animal Studies

Our animal experiments were conducted following the National Institutes of Health guide for the care and use of Laboratory animals and approved by the Ethics Committee of the Institutional Animal Care and Use Committee of Tongji Medical College, Huazhong University of Science and Technology (Wuhan, China; IACUC, S2393). For brain metastasis experiments, male BALB/c nude mice (6- to 8-week-old; Beijing Vital River Laboratory Animal Technology Co., Ltd; Beijing, China)

were raised in a specific pathogen-free (SPF) laboratory of the Animal Experiment Center. The mice were randomly divided into two groups. In the irradiated group, mice were treated with 3 Gy*2f of irradiation to the whole brain and raised for 1 week (the duration of preventive irradiation is determined by the inflammatory response and the level of miR-9 in the brain microenvironment). Subsequently, 100 μL PBS containing 2×10^5 luciferase-labeled A549-F3 cells was injected into the left cardiac ventricle of each mouse. At the end of the experiment, mice were sacrificed and examined for brain metastases.

Intravital Imaging and Analysis

Mice received an intraperitoneal injection of 150μl of 1.5% D-luciferin and anaesthetized with 1.5% sodium pentobarbital. Imaging was completed with a Xenogen IVIS system (Caliper) coupled to Living Image Acquisition and Analysis software (Xenogen). For BLI plots, photon flux was calculated for each mouse by using a rectangular region of interest encompassing the mouse's thorax.

Statistical Analyses

Statistical calculations were performed using GraphPad Prism 8.0.1 (GraphPad Software, CA, USA). Statistical comparisons between experimental groups were performed with a two-tailed Student's *t*-test. Data are shown as mean ± SD. P <0.05 was considered indicative of significant findings. *P < 0.05, **P < 0.01, ***P < 0.001, ****P < 0.0001, *****P < 0.00001

Results
Irradiated Microglia Exhibited M1-Type Polarization and Hampered A549 Cells MET Transition

To explore the impact of irradiation on microglial phenotype, CHME5 cells were treated with 0, 2, 3, 4 Gy of irradiation. Then, the mRNA levels of iNOS and Arg1, the phenotype markers for M1 and M2 microglial were measured, respectively. There was a noticeable up-regulation in iNOS expression and down-regulation of Arg1 expression in irradiated microglia, particularly in the group treated with 3 Gy (Figure 1A). Western Blot analysis revealed different levels of iNOS or Arg1 with different dose gradients (Supplementary Figure 2). We can see obvious up-regulation of iNOS and IL1B (M1 markers) expression after treatment with 3 Gy irradiation

(Figure 1B). Further analysis showed that the effects of irradiation were extremely obvious at 48 h using qRT-PCR and Western Blot (Figure 1C and D). Results of immuno-fluorescence staining with iNOS showed obvious M1 activated microglia at 48h after irradiation (Figure 1E).

Next, we explored the role of irradiated M1 microglia on the phenotypical modulation of NSCLC cells. The expression of E-cadherin and vimentin in A549 cells was analyzed by Western Blot, both of which are vital markers of epithelial/mesenchymal phenotype. In the group with control culture media, the mesenchymal phenotype A549 cells quickly reversed into epithelial type with high E-cadherin and low vimentin expression. In contrast, in the group treated with irradiated CHME5 supernatant, A549 cells retained their mesenchymal phenotype with low E-cadherin and high vimentin expression. Introduction to these groups of CHME5 supernatant without irradiation or U87 supernatant (negative control group) did not affect the observed phenotype changes compared with the control group (Figure 1F).

Both Intra and Extracellular miR-9 Level Upregulated in Irradiation-Induced M1 Microglia

Recent studies indicated that microRNAs played crucial roles in the regulation of EMT/MET process.[30,31] Thus, we analyzed microRNA expression in the LPS-treated group and control group. miR-9 levels increased dramatically in LPS-induced M1 microglia (Figure 2A). Among the up-regulated miRNAs, miRNA-9 attracted our attention for its important role in EMT. We confirmed that the level of miR-9 was significantly elevated in irradiated CHME5 and HMO6 cells (3 Gy and 3 Gy*2f), when compared with non-irradiated microglia, both intracellularly (Figure 2B and D) and extracellularly (Figure 2C and E). These results showed that miR-9 expression was up-regulated in irradiated microglia and secreted into the extracellular space, suggesting that miR-9 secreted by irradiated microglia may play an important role in inducing a mesenchymal phenotype in metastatic A549 cells.

Intracellular Level of miR-9 in A549 Cell Lines Unregulated by Irradiated M1-Type Microglia

To confirm the effects of miR-9 produced by irradiated M1 microglia on the MET process, we modulated the expression of miR-9 in A549 or brain metastatic A549-F3 cells,
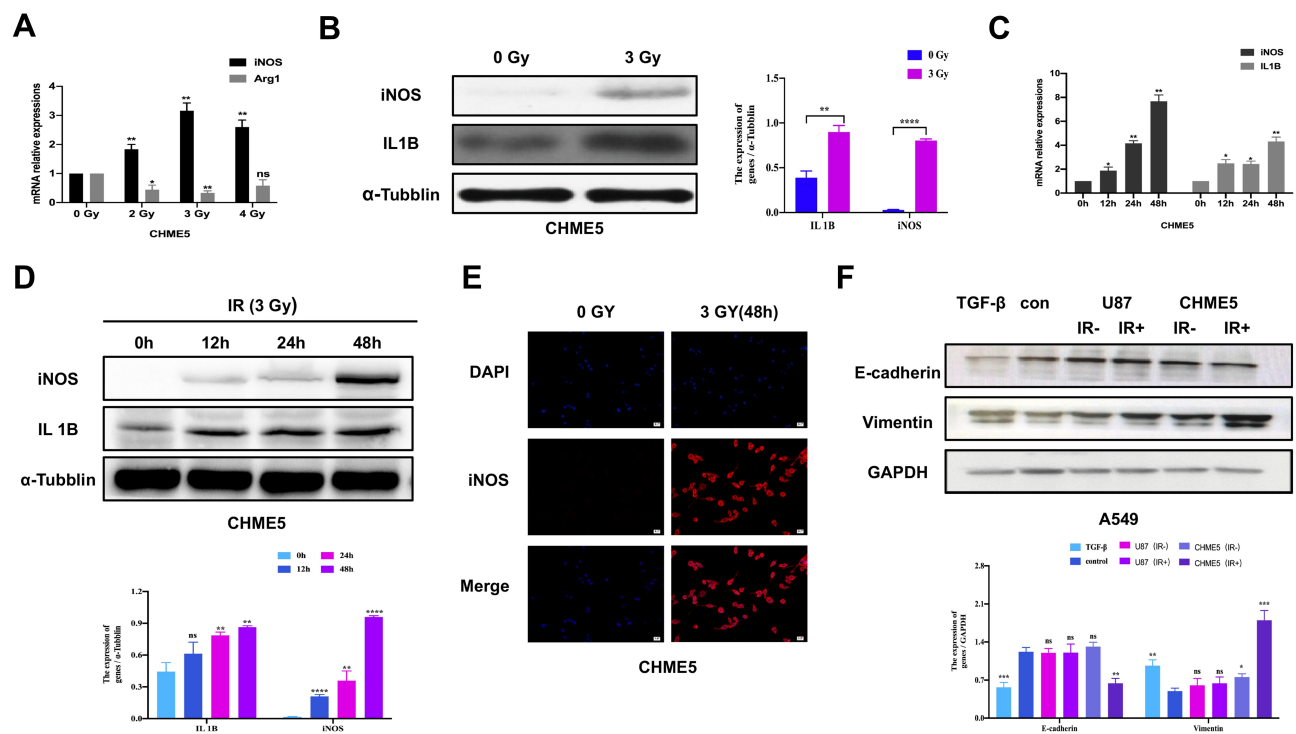
Figure 1 Irradiated microglia exhibited M1-type polarization and hampered A549 cells MET transition. (**A**) qRT-PCR results of iNOS and IL10 mRNA expression in CHME5 cells after 0, 2, 3, 4 Gy irradiation. (**B**) Protein expression of Arg1 and iNOS in CHME5 cells after 0, 2, 3, 4 Gy irradiation, α-tubulin was used as positive control. (**C**) qRT-PCR results of iNOS and IL1B mRNA expression in CHME5 cells at different time points (0h; 12h; 24h; 48h) after 3 Gy irradiation. (**D**) Protein expression of IL1B and iNOS in CHME5 cells at different time points (0h; 12h; 24h; 36h; 48h) after 3 Gy irradiation. α-Tubulin was used as positive control. (**E**) Immunofluorescence staining analysis was employed to detect the iNOS (red) in CHME5 cells with or without irradiation (3 Gy for 48h). The blue signal represents the DAPI-stained nuclei. Magnification was 200×. (**F**) Protein expression of E-cadherin and vimentin in A549 cells. All groups of A549 cells were firstly treated with TGF-β1 (2.5μg/mL). Then, controlled culture media, cell culture supernatant of U87 with or without irradiation (IR+/IR-), cell culture supernatant of CHME5 with or without irradiation (IR+/IR-), were added into those TGF-β1-treated A549 cells, respectively. IR: irradiation. Data are mean ± SD. ns, P>0.05, *P<0.05, **P<0.01.***P<0.001, ****P<0.0001.

using an miR-9 mimic and inhibition of plasmid transduction (Figure 3A and C). Levels of intracellular miR-9 were detected via qRT-PCR in each of three groups: negative control, up-expression, and down-expression group. Significantly elevated/decreased miR-9 levels were detected in the up/down group, respectively, confirming the success of in vitro miR-9 expression modulation in A549 and A549-F3 cells (Figure 3B and D).

Next, we added irradiated or non-irradiated microglia culturing supernatant into A549 and A549-F3 cells transfected with negative (neg)/miR-9 mimic (up)/miR-9 inhibition (down) plasmid, respectively, observing the highest level of miR-9 in miR-9 mimic group treated with irradiated conditioned medium. In contrast, the lowest miR-9 level was detected in the miR-9 inhibition group, where the non-irradiated microglia supernatant was added (Figure 3E and F). When the miR-9 inhibition A549/A549-F3 group was treated with irradiated microglia supernatant, their intracellular levels of miR-9 were significantly higher than those in the miR-9 inhibition group

treated with non-irradiated microglia supernatant. This result suggests that irradiated M1 microglia increased their production and secretion of miR-9; and so, the level of miR-9 in A549 and A549-F3 was increased. This absorbed miR-9 might play a role in reducing NSCLC brain metastasis.

Irradiated M1 Type Microglia Inhibited the MET via miR-9/CDH1 Axis

To explore the influence of miR-9 levels on phenotypic conversions of A549 and A549-F3 cells, we conducted Western blot analysis. In Figure 4A, groups with controlled culture media and negative plasmid the mesenchymal phenotype A549 cells quickly reversed into epithelial-type with high E-cadherin and low vimentin expression. In contrast, groups with up-regulated miR-9 retained their mesenchymal phenotype (low E-cadherin and high vimentin expression). Among groups with up-regulated miR-9, those treated with irradiated microglia supernatant retained the most typical mesenchymal phenotype. Meanwhile, miR-9 downregulation
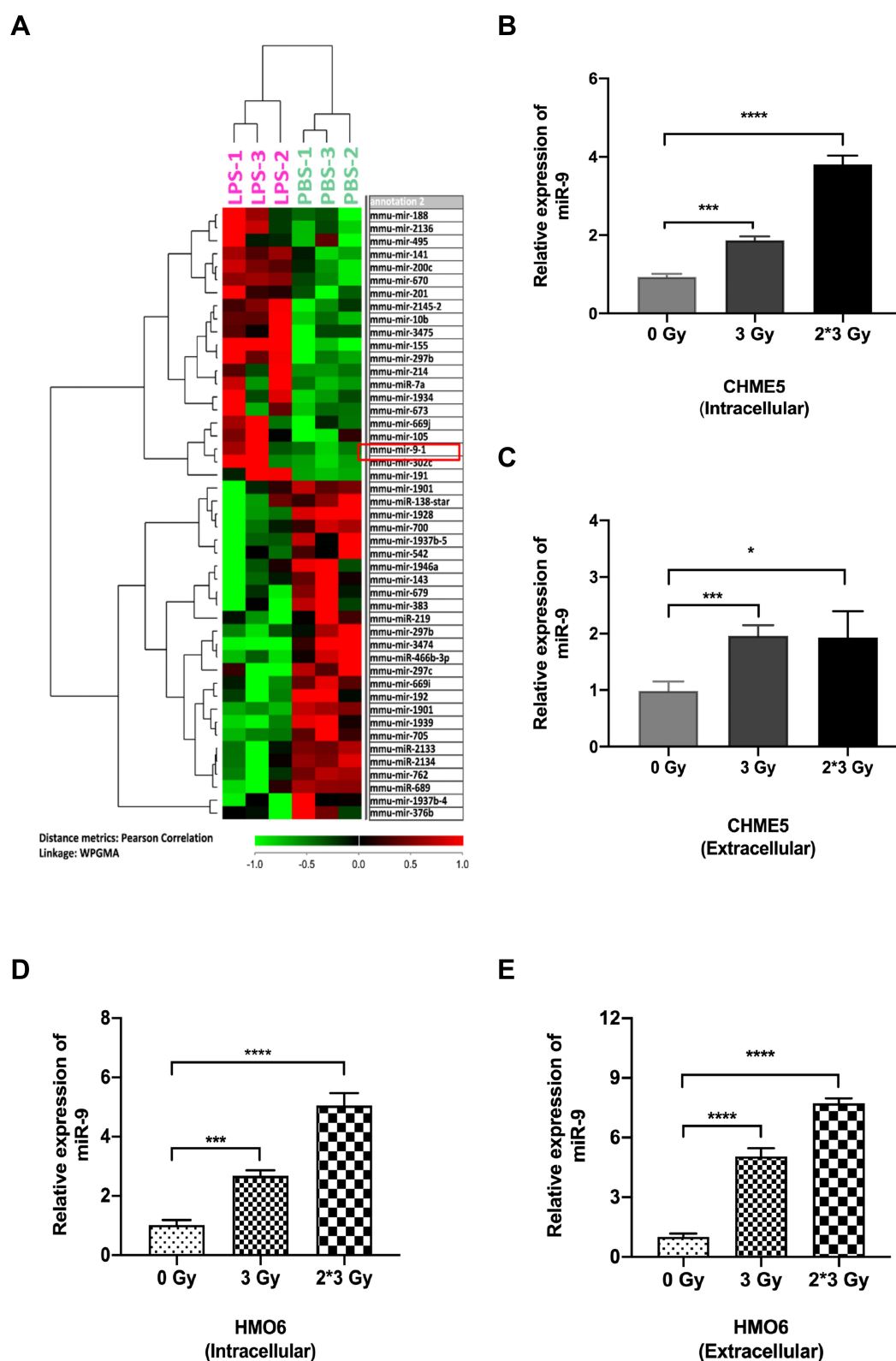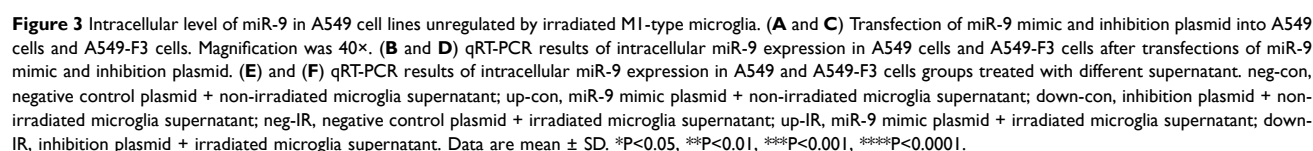
Figure 2 Both intra- and extracellular miR-9 level upregulated in irradiation-induced M1 microglia. (**A**) Heat map of miRNA microarray data shows differentially expressed miRNA pattern between LPS-treated and PBS-treated microglia. Red indicates relatively up-regulated genes. Green indicates relatively down-regulated genes. The red box in panel A showed that miR-9 was significantly upregulated in LPS-treated M1 microglia. (**B**) qRT-PCR results of intracellular miR-9 expression in CHME5 cells after 0 Gy, 3 Gy, 3 Gy*2f, irradiation. (**C**) qRT-PCR results of extracellular miR-9 expression in CHME5 cells after 0 Gy, 3 Gy, 3 Gy*2f, irradiation. (**D**) qRT-PCR results of intracellular miR-9 expression in HMO6 cells after 0 Gy, 3 Gy, 3 Gy*2f, irradiation. (**E**) qRT-PCR results of extracellular miR-9 expression in HMO6 cells after 0 Gy, 3 Gy, 3 Gy*2f, irradiation. Data are mean ± SD. ns, P>0.05, *P<0.05, ***P<0.001; ****P<0.0001.

Figure 3 Intracellular level of miR-9 in A549 cell lines unregulated by irradiated M1-type microglia. (**A** and **C**) Transfection of miR-9 mimic and inhibition plasmid into A549 cells and A549-F3 cells. Magnification was 40×. (**B** and **D**) qRT-PCR results of intracellular miR-9 expression in A549 cells and A549-F3 cells after transfections of miR-9 mimic and inhibition plasmid. (**E**) and (**F**) qRT-PCR results of intracellular miR-9 expression in A549 and A549-F3 cells groups treated with different supernatant. neg-con, negative control plasmid + non-irradiated microglia supernatant; up-con, miR-9 mimic plasmid + non-irradiated microglia supernatant; down-con, inhibition plasmid + non-irradiated microglia supernatant; neg-IR, negative control plasmid + irradiated microglia supernatant; up-IR, miR-9 mimic plasmid + irradiated microglia supernatant; down-IR, inhibition plasmid + irradiated microglia supernatant. Data are mean ± SD. *P<0.05, **P<0.01, ***P<0.001, ****P<0.0001.
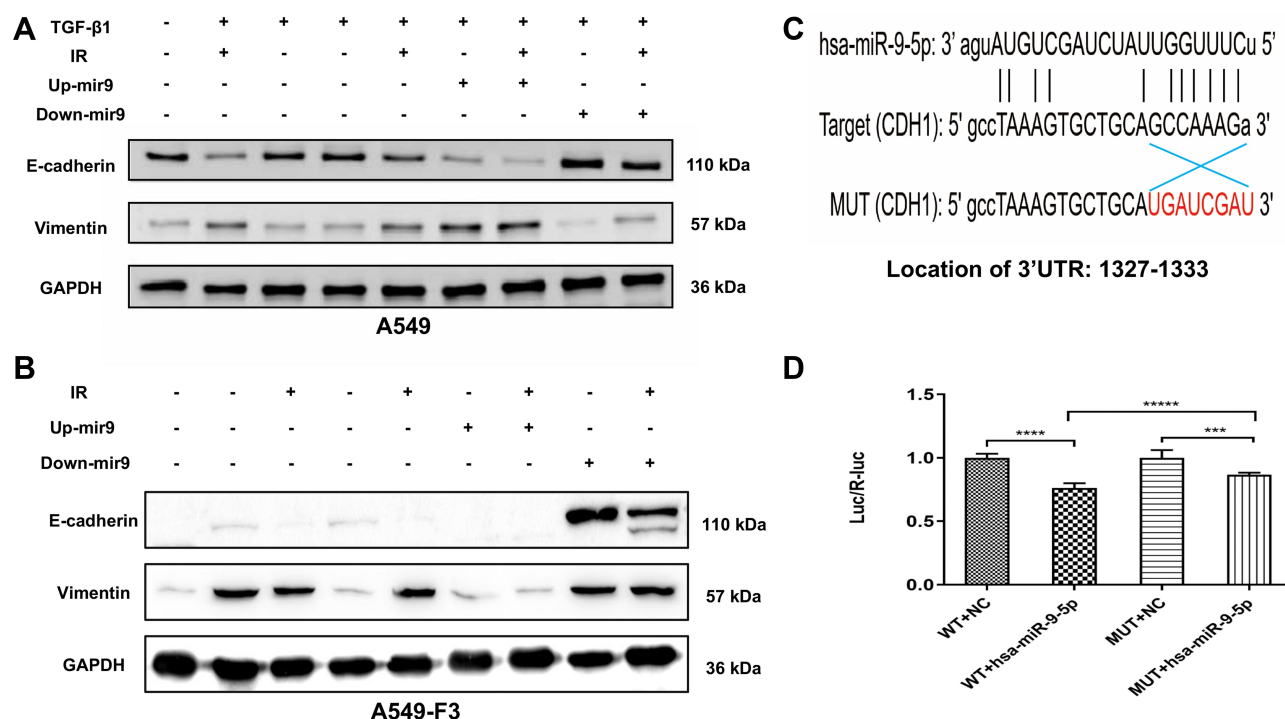
Figure 4 Irradiated M1 type microglia inhibited the MET via miR-9/CDH1 axis. (**A** and **B**) Protein expression of E-cadherin and vimentin in A549 cells and A549-F3 cells. All groups of A549 cells transfected with negative control, miR-9 mimics (up+), miR-9 inhibition (down+) plasmid were firstly treated with TGF-β1 (TGF-β1+). Then, controlled culture media, cell culture supernatant of CHME5 cells with or without irradiation (IR+/IR-), were added into those TGF-β1-treated A549 cells or A549-F3 cells, respectively. (**C**) Schematic representation of the 3′-UTR of *CDH1* with the predicted target site for miR-9-5p. The mutant site of *CDH1* 3′-UTR is indicated as red font (without line). (**D**) Relative luciferase activity was assayed in different groups. H15279: WT; H15280: MUT; NC: scramble miRNA mimic; miR-9: miR-9-5p mimic. Data are mean ± SD. ***P<0.001, ****P<0.0001, *****P<0.00001.

could promote E-cadherin expression. Furthermore, A549 cells with down-regulated miR-9 treated with non-irradiated microglia supernatant transformed into the most typical epithelial phenotype (the highest E-cadherin and the lowest Vvimentin expression). Consistent with the observations above, A549-F3 cells transfected with down-regulated miR-9 plasmid were able to develop an epithelial phenotype, while irradiated microglia supernatant could inhibit the MET process to keep the A549-F3 cells in a mesenchymal state. Meanwhile, A549-F3 cells with up-regulated miR-9 treated with irradiated CHME5 supernatant maintained the most typical mesenchymal phenotype (Figure 4B).

Given that, miRNAs could inhibit gene expression by binding to the 3′UTR of respective RNAs,[32] WT and MUT of *CDH1* 3′UTR-driven luciferase vectors were respectively cotransfected with NC or miR-9-5p mimics into 293T cells (Figure 4C). Results indicated cotransfection with miR-9-5p mimics and WT *CDH1* 3′-UTR caused inhibition of luciferase activity. Moreover, cotransfection of miR-9-5p mimics and MUT *CDH1* 3′-UTR had no effects on luciferase activity (Figure 4D). These findings point to *CDH1* being the target of miR-9.

Low-Dose Irradiation Reduced Brain Metastases of A549-F3 Cells in Brain Mice Model

To confirm the effects of irradiation on NSCLC-BM in vivo, we selected 7 days after irradiation to inject tumor cells for the higher level of miR-9 (Supplementary Figure 3). We use bioluminescence imaging (BLI) to assess the incidence rate of BM in a mouse model (Figure 5A and B). BM incidence was reduced in irradiated mice (40%, n=10), when compared to the control group (70%, n=10) (Figure 5C). There are significant differences between the two groups by analysis of the photon flux (Figure 5D). Furthermore, irradiation increased miR-9 levels in mice brain microenvironment (Figure 5E). These findings suggest that, in a mouse model, low-dose irradiation reduces A549-F3 cells-mediated brain metastases, possibly by elevating miR-9 expression levels, which inhibit the MET process of tumor cells in the brain microenvironment. The mechanism that cranial irradiation (3 Gy) might prevent NSCLC-BM is shown in Figure 5F.
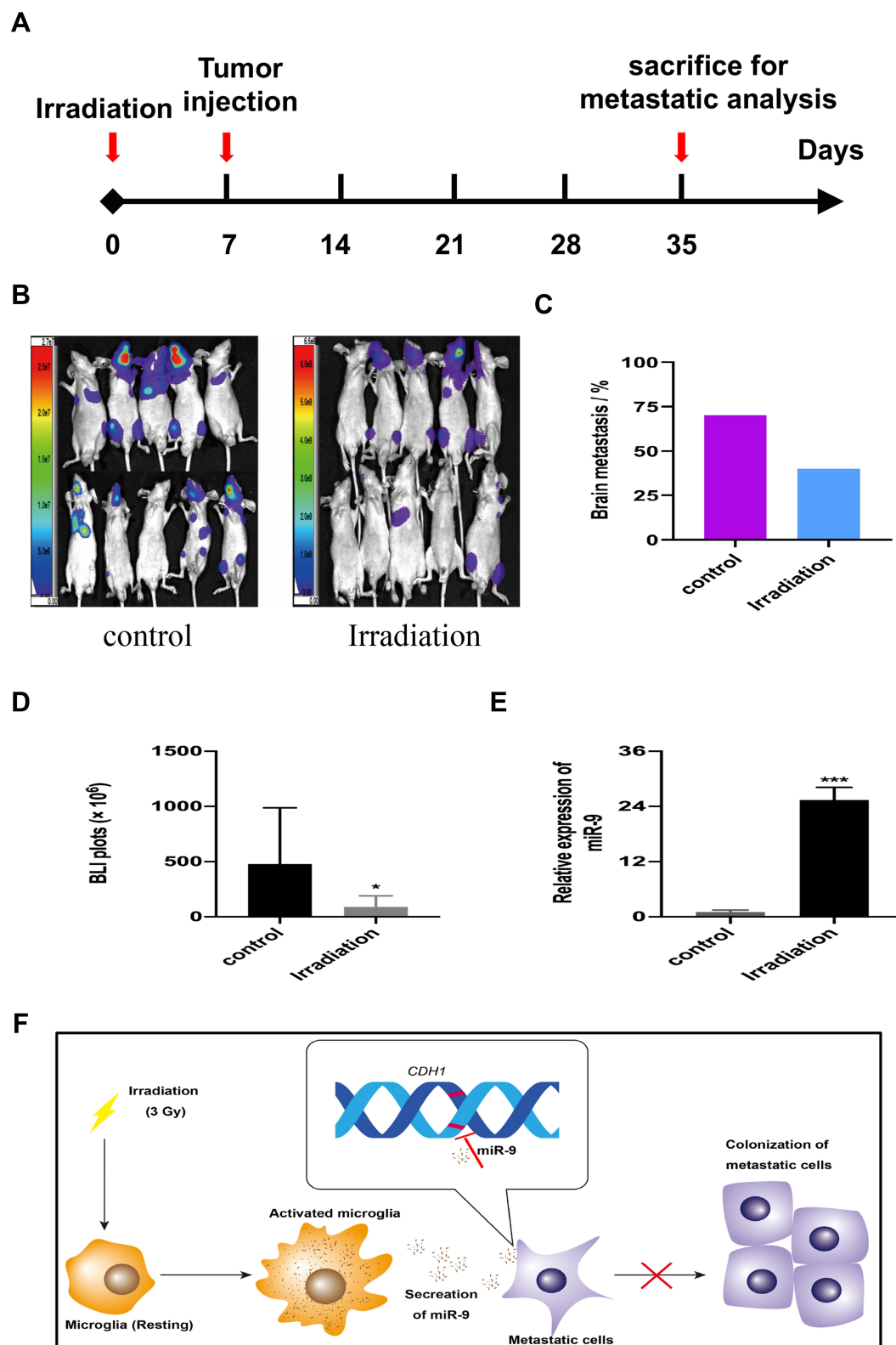
Figure 5 Low-dose irradiation reduced brain metastases of A549-F3 cells in brain mice model. (**A**) Schematic diagram illustrates the treatment schedule of irradiation. (**B**) Brain metastases were determined by bioluminescence imaging in control and irradiated group. (**C**) Histogram showed incidence of brain metastasis in control and irradiated group. (**D**) Photon flux detected from brain metastatic focus in control and irradiated group. (**E**) qRT-PCR results of miR-9 from brain tissue of mouse treated with or without irradiation. (**F**) The mechanism that cranial irradiation (3 Gy) might prevent NSCLC-BM. In the brain, microglia activated by 3 Gy irradiation and secreted more miR-9, which could maintain A549 cell lines with mesenchymal phenotype. Thereby, activated microglia decreased localization capabilities of NSCLC brain metastatic cells and reduced brain metastases. Data are mean ± SD. *P<0.05, ***P<0.001.

Discussion

In this study, we showed a significant shift towards M1 microglia phenotype after irradiation. Moreover, M1 microglia inhibited the MET process of A549 cell lines, a crucial step in their capacity for adhesion to and colonization of distant organs, in particular, the brain. MiRNA array analysis revealed up-regulated expression of miR-9 in M1 microglia. In addition, increased miR-9 secreted by irradiated M1 microglia played an important role in inhibition of the MET process. Finally, miR-9 exerted these effects by targeting *CDH1*, a gene vital to this process. Evidence from a mouse model supported the effects of irradiation-induced miR-9 elevation on lowering the incidence of brain metastasis in A549-F3 cells.

It has been well established that microglia localizing in brain parenchymal are the main cellular constituent that are involved in brain innate immunity.[33] They detect "danger signals" including presence of infectious agent, toxins and cell damage among others, using danger-associated-molecular-pattern receptors (DAMP) and trigger inflammatory responses.[11,16] Here, our findings are consistent with previous studies that irradiation promoted M1 microglia activation and anti-metastatic effects.[12] Concurrently, numerous studies have suggested that the pro-inflammatory status of M1 microglia showed anti-tumoral capacity via improved antigen-presenting capabilities and direct suppression of tumor growth.[34,35] This study revealed a novel mechanism of inhibitory effects on NSCLC cells localization, presumably by promoting miR-9 production and secretion from irradiated M1 microglia.

Recent studies have indicated that miR-9 exhibits anti-tumor effects by inhibiting tumor cell motility.[36] Specifically, Ben-Hamo et al demonstrated that overexpression of miR-9 in glioblastoma hampered tumor cell mobility, possibly via inhibition of the MAPK pathway, which subsequently disrupted cellular actin cytoskeleton organization.[37] In addition, Xu et al showed that ectopic expression of miR-9 in melanoma cells suppressed the tumor capacity of migration and invasion.[38,39] These authors identified the downstream target gene NRP1, negatively regulated by miR-9, as responsible for the change in motility of tumor cells.[40] Meanwhile, growing evidences have indicated that miR-9 plays a vital role in regulating the MET process and tumor cell metastasis.[41] In our research, through high-throughput micro-RNA profiling analysis, we observed significant miR-9 up-regulation in irradiated microglia. This increased miR-9 expression within A549 cell lines, in turn, promoted their mesenchymal phenotype. Eventually, decreased expression of epithelial molecules in metastatic tumor cells hampered their localizing capacity in the brain.

However, we must point out that our research has some limitations. On one hand, we only got preliminary results and have not verified the possibility of the target as an intervention treatment. For another, the present findings are based on cellular and animal models, while elucidating the molecular mechanism of irradiated effects on brain metastasis in NSCLC patients requires further studies involving human subjects. Furthermore, since PCI is routinely used for SCLC patients that we should explore whether this model also applies to the SCLC model.

Conclusion

Overall, we found significant "M1" polarization shifting of microglia after irradiation treatment. We demonstrated irradiation-induced M1-type microglia significantly modulate metastatic A549 cell lines into mesenchymal phenotype through up-regulating and secreting of miR-9, which eventually shifted tumor cell into mesenchymal phenotype and further decreased localization capabilities in brain. Our study firstly demonstrated that irradiated microglia modulated tumor cell MET process via miR-9/*CDH1* axis, providing new insights into PCI's mechanism. It might inform further studies on irradiation effects to tumor microenvironment. Clinically, miR-9 expression might act as a predictive biomarker for brain metastasis in NSCLC patients. Moreover, treatments targeting the miR-9 pathway combined with radiotherapy might help reduce the risk of brain metastasis, providing novel perspectives for effective anti-metastatic therapies.

Abbreviations

SCLC, small cell lung cancer; NSCLC, non-small cell lung cancer; BM, brain metastasis; PCI, prophylactic cranial irradiation; IR, ionizing radiation; EMT, epithelial-to-mesenchymal transition; MET, mesenchymal-to-epithelial transition; DMEM, Dulbecco's minimal essential media; RMA, robust multichip analysis; LPS, lipopolysaccharides; FBS, fetal bovine serum; PBS, phosphate-buffered saline; PCR, polymerase chain reaction; DAPI, diamidino-phenylindole; WT, wild type; MUT, mutant type; BLI, bioluminescence imaging; UTR, untranslated regions; DAMP, danger-associated-molecular-pattern receptors; miRNAs, microRNAs; SD, standard deviation.

Acknowledgments

Disclosure

The authors declare that they have no competing interests in this work.

References

1. Bade BC, Dela Cruz CS. Lung cancer 2020: epidemiology, etiology, and prevention. *Clin Chest Med*. 2020;41(1):1–24.
2. Siegel RL, Miller KD, Jemal A. Cancer statistics, 2019. *CA Cancer J Clin*. 2019;69(1):7–34.
3. Yousefi M, Bahrami T, Salmaninejad A, Nosrati R, Ghaffari P, Ghaffari SH. Lung cancer-associated brain metastasis: molecular mechanisms and therapeutic options. *Cell Oncol*. 2017;40 (5):419–441.
4. Tabouret E, Chinot O, Metellus P, Tallet A, Viens P, Goncalves A. Recent trends in epidemiology of brain metastases: an overview. *Anticancer Res*. 2012;32(11):4655–4662.
5. Achrol AS, Rennert RC, Anders C, et al. Brain metastases. *Nat Rev Dis Primers*. 2019;5(1):5.
6. Li QX, Zhou X, Huang TT, et al. The Thr300Ala variant of ATG16L1 is associated with decreased risk of brain metastasis in patients with non-small cell lung cancer. *Autophagy*. 2017;13 (6):1053–1063.
7. Nakahara Y, Sasaki J, Fukui T, et al. The role of prophylactic cranial irradiation for patients with small-cell lung cancer. *Jpn J Clin Oncol*. 2018;48(1):26–30.
8. Bloom BC, Augustyn A, Sepesi B, et al. Prophylactic cranial irradiation following surgical resection of early-stage small-cell lung cancer: a review of the literature. *Front Oncol*. 2017;7:228.
9. Aupérin A, Arriagada R, Pignon J-P, et al. Prophylactic cranial irradiation for patients with small-cell lung cancer in complete remission. *N Engl J Med*. 1999;341(7):476–484.
10. Sun A, Hu C, Wong SJ, et al. Prophylactic cranial irradiation vs observation in patients with locally advanced non-small cell lung cancer: a long-term update of the NRG oncology/RTOG 0214 Phase 3 randomized clinical trial. *JAMA Oncol*. 2019;5(6):847–855.
11. Lumniczky K, Szatmari T, Safrany G. Ionizing radiation-induced immune and inflammatory reactions in the brain. *Front Immunol*. 2017;8:517.
12. Morganti JM, Jopson TD, Liu S, Gupta N, Rosi S. Cranial irradiation alters the brain's microenvironment and permits CCR2+ macrophage infiltration. *PLoS One*. 2014;9(4):e93650.
13. Zhang L, Zhang S, Yao J, et al. Microenvironment-induced PTEN loss by exosomal microRNA primes brain metastasis outgrowth. *Nature*. 2015;527(7576):100–104.
14. Wu S-Y. The roles of microglia macrophages in tumor progression of brain cancer and metastatic disease. *Frontiers Biosci*. 2017;22 (10):1805–1829.
15. Kang Y, Jin Y, Li Q, Yuan X. Advances in lung cancer driver genes associated with brain metastasis. *Front Oncol*. 2020;10:606300.
16. Eggen BJL, Raj D, Hanisch UK, Boddeke HWGM. Microglial phenotype and adaptation. *J Neuroimmune Pharmacol*. 2013;8 (4):807–823.
17. Cheray M, Joseph B. Epigenetics control microglia plasticity. *Front Cell Neurosci*. 2018;12.
18. Wei J, Gabrusiewicz K, Heimberger A. The controversial role of microglia in malignant gliomas. *Clin Dev Immunol*. 2013;2013:285246.
19. Yu H, Pardoll D, Jove R. STATs in cancer inflammation and immunity: a leading role for STAT3. *Nat Rev Cancer*. 2009;9(11):798–809.
20. Annovazzi L, Mellai M, Bovio E, Mazzetti S, Pollo B, Schiffer D. Microglia immunophenotyping in gliomas. *Oncol Lett*. 2018;15 (1):998–1006.
21. Califano R, Kerr K, Morgan RD, et al. Immune checkpoint blockade: a new era for non-small cell lung cancer. *Curr Oncol Rep*. 2016;18(9):59.
22. Acharyya S, Oskarsson T, Vanharanta S, et al. A CXCL1 paracrine network links cancer chemoresistance and metastasis. *Cell*. 2012;150 (1):165–178.
23. Jolly MK, Boareto M, Huang B, et al. Implications of the hybrid epithelial/mesenchymal phenotype in metastasis. *Front Oncol*. 2015;5:155.
24. Davis FM, Stewart TA, Thompson EW, Monteith GR. Targeting EMT in cancer: opportunities for pharmacological intervention. *Trends Pharmacol Sci*. 2014;35(9):479–488.
25. Mirzaei H, Masoudifar A, Sahebkar A, et al. MicroRNA: a novel target of curcumin in cancer therapy. *J Cell Physiol*. 2018;233 (4):3004–3015.
26. Gunasinghe NPAD, Wells A, Thompson EW, Hugo HJ. Mesenchymal–epithelial transition (MET) as a mechanism for metastatic colonisation in breast cancer. *Cancer Metastasis Rev*. 2012;31 (3–4):469–478.
27. Legras A, Pécuchet N, Imbeaud S, et al. Epithelial-to-mesenchymal transition and MicroRNAs in lung cancer. *Cancers*. 2017;9:12.
28. Yi M, Liu B, Tang Y, Li F, Qin W, Yuan X. Irradiated human umbilical vein endothelial cells undergo endothelial-mesenchymal transition via the Snail/miR-199a-5p axis to promote the differentiation of fibroblasts into myofibroblasts. *Biomed Res Int*. 2018;2018:1–10.
29. Nyl LY, Li Z, Min X. DNMT3A R882 mutation is associated with elevated expression of MAFB and M4-M5 immunophenotype of acute myeloid. *Leuk Lymphoma*. 2015;56(10):9.
30. Park YR, Lee ST, Kim SL, et al. Down-regulation of miR-9 promotes epithelial mesenchymal transition via regulating anoctamin-1 (ANO1) in CRC cells. *Cancer Genet*. 2019;231–232:22–31.
31. Zhou B, Xu H, Xia M, et al. Overexpressed miR-9 promotes tumor metastasis via targeting E-cadherin in serous ovarian cancer. *Front Med*. 2017;11(2):214–222.
32. Bartel DP. MicroRNAs: genomics, biogenesis, mechanism, and function. *Cell*. 2004;116(2):281–297.
33. Wei J, Chen P, Gupta P, et al. Immune biology of glioma-associated macrophages and microglia: functional and therapeutic implications. *Neuro Oncol*. 2020;22(2):180–194.
34. Sarkar S, Döring A, Zemp FJ, et al. Therapeutic activation of macrophages and microglia to suppress brain tumor-initiating cells. *Nat Neurosci*. 2013;17(1):46–55.
35. Lahmar Q, Keirsse J, Laoui D, Movahedi K, Van Overmeire E, Van Ginderachter JA. Tissue-resident versus monocyte-derived macrophages in the tumor microenvironment. *Biochimica Et Biophysica Acta (BBA) Rev Cancer*. 2016;1865(1):23–34.
36. Zhu L, Chen H, Zhou D, et al. MicroRNA-9 up-regulation is involved in colorectal cancer metastasis via promoting cell motility. *Med Oncol*. 2012;29(2):1037–1043.
37. Rotem Ben-Hamo AZ, Cohen H, Efroni S. hsa-miR-9 controls the mobility behavior of Glioblastoma cells via regulation of MAPK14 signaling elements. *Onco Targets Ther*. 2016;7:12.

38. Xu XZ, Li XA, Luo Y, Liu JF, Wu HW, Huang G. MiR-9 promotes synovial sarcoma cell migration and invasion by directly targeting CDH1. *Int J Biochem Cell Biol.* 2019;112:61–71.

39. Han Y, Liu Y, Fu X, et al. miR-9 inhibits the metastatic ability of hepatocellular carcinoma via targeting beta galactoside alpha-2,6-sialyltransferase 1. *J Physiol Biochem.* 2018;74(3):491–501.

40. Xu D, Chen X, He Q, Luo C. MicroRNA-9 suppresses the growth, migration, and invasion of malignant melanoma cells via targeting NRP1. *Onco Targets Ther.* 2016;9:7047–7057.

41. Wang WX, Yu HL, Liu X. MiR-9-5p suppresses cell metastasis and epithelial-mesenchymal transition through targeting FOXP2 and predicts prognosis of colorectal carcinoma. *Eur Rev Med Pharmacol Sci.* 2019;23(15):6467–6477.